A BEM for Transient Anisotropic Diffusion Convection Equation of Variable Coefficients

Mohammad Ivan Azis

***Abstract*—This article addresses challenges associated with anisotropic functionally graded media that are governed by the transient diffusion-convection equation. The authors seek to obtain numerical solutions for these problems by utilizing a combination of Laplace transform and boundary element method. To achieve this, a boundary integral equation is derived and a standard boundary element method is used to obtain numerical solutions, which are then inversely transformed using the Stehfest formula to obtain solutions in the time variable. The problems studied include those involving compressible or incompressible flow and media with quadratic, exponential, and trigonometric gradients. The findings suggest that the approach used to transform the variable coefficients equation into the constant coefficients equation is valid and the mixed Laplace transform and boundary element method is a simple and effective means of obtaining numerical solutions. The accuracy of the numerical solutions is also confirmed, and the impact of material anisotropy and inhomogeneity on the solutions is highlighted, suggesting that accounting for these factors is crucial for experimental studies. Additionally, the symmetry of solutions for symmetric problems is also verified for further validation of the numerical solutions.**

***Index Terms*—diffusion convection equation, anisotropic, transient, variable coefficients, boundary element method**

I. Introduction

The diffusion convection (DC) equation has multiple applications in various fields, such as biology, ecology, engineering, and medicine. Several studies have been carried out to find its numerical solution. Some of these studies, (for example [1]–[4]) considered the DC equation with constant coefficients for homogeneous media. Whereas, [5]–[10] focused on the DCR equation with variable velocity for inhomogeneous media. Some other studies on problems of inhomogeneous anisotropic media for several types of governing equations had been done (see for examples, [11]–[14].

This paper is intended to extend the recently published works [15]–[18] on the steady DC equation to the transient DC equation for anisotropic functionally graded materials of the form

$$\frac{\partial}{\partial x_i}\left[d_{ij}(\mathbf{x})\frac{\partial c(\mathbf{x},t)}{\partial x_j}\right]-\frac{\partial}{\partial x_i}\left[v_i(\mathbf{x})\,c(\mathbf{x},t)\right] = \psi(\mathbf{x})\frac{\partial c(\mathbf{x},t)}{\partial t} \quad i,j=1,2 \tag{1}$$

Equation (1) provides a wider class of problems since it applies for *anisotropic and inhomogeneous* media but nonetheless covers the case of isotropic diffusion taking place when $d_{11}=d_{22}, d_{12}=0$ and also the case of homogeneous media which occurs when the coefficients $d_{ij}(\mathbf{x})$, $v_i(\mathbf{x})$ and $\psi(\mathbf{x})$ are constant. The class of inhomogeneity that will be covered in (1) is different to those considered in [5]–[10].

Within the Cartesian frame Ox_1x_2 we will consider initial boundary value problems governed by (1) where $\mathbf{x}=(x_1,x_2)$. The coefficient $[d_{ij}]$ is a symmetric matrix with positive determinant. In (1) the summation convention holds for repeated indices so that explicitly equation (1) takes the form

$$\frac{\partial}{\partial x_1}\left(d_{11}\frac{\partial c}{\partial x_1}\right)+\frac{\partial}{\partial x_1}\left(d_{12}\frac{\partial c}{\partial x_2}\right)+\frac{\partial}{\partial x_2}\left(d_{12}\frac{\partial c}{\partial x_1}\right) +\frac{\partial}{\partial x_2}\left(d_{22}\frac{\partial c}{\partial x_2}\right)-\frac{\partial}{\partial x_1}(v_1c)-\frac{\partial}{\partial x_2}(v_2c)=\psi\frac{\partial c}{\partial t}$$

In recent times, functionally graded materials (FGMs) have gained significant attention, and many studies have been conducted on their applications for various purposes, as documented by Zhou et al. [19], Zhou et al. [20]. Typically, FGMs are described as inhomogeneous materials whose specific characteristics, such as thermal conductivity, hardness, toughness, ductility, corrosion resistance, etc., change in a continuous manner over space. The coefficients d_{ij}, v_i, ψ in (1) vary continuously and represent specific characteristics of the medium of interest, thus making equation (1) relevant for FGMs.

II. The initial boundary value problem

By knowing the coefficients $d_{ij}(\mathbf{x}), v_i(\mathbf{x}), \psi(\mathbf{x})$ we will seek solutions $c(\mathbf{x},t)$ and its derivatives which are valid for time interval $t\geq 0$ and in a region Ω in R^2 with boundary $\partial\Omega$ which consists of a finite number of piecewise smooth curves. On the boundary $\partial\Omega_1$ the dependent variable $c(\mathbf{x},t)$ is given, and

$$P(\mathbf{x},t)=d_{ij}(\mathbf{x})\frac{\partial c(\mathbf{x},t)}{\partial x_i}n_j \tag{2}$$

is specified on $\partial\Omega_2$ where $\partial\Omega=\partial\Omega_1\cup\partial\Omega_2$ and $\mathbf{n}=(n_1,n_2)$ represents the outward pointing normal to $\partial\Omega$. The initial condition is

$$c(\mathbf{x},0)=0 \tag{3}$$

III. The boundary integral equation

To solve the variable coefficient equation (1), the first step is to convert it into a constant coefficient equation, and then apply a Laplace transform. By doing so, a boundary integral equation can be formulated with the transformed constant coefficient equation, using the Laplace transform dummy variable s and the position vector $\mathbf{x}$. The boundary integral equation is then solved through the application of the standard boundary element method (BEM). Afterward, the

Manuscript received March 4, 2023; revised June 26, 2023.

This work was supported in part by Hasanuddin University and Ministry of Education, Culture, Research, and Technology of Indonesia.

M. I. Azis is a professor at the Department of Mathematics, Hasanuddin University, Makassar 90245, Indonesia (phone: 62-811-466-230; e-mail: ivan@unhas.ac.id).

solution c and its derivatives can be obtained for all $(\mathbf{x}, t)$ in the domain using an inverse Laplace transform. The Stehfest formula is used to implement the numerical calculation of the inverse Laplace transform.

We restrict the coefficients d_{ij}, v_i, ψ to be of the form

$$d_{ij}(\mathbf{x}) = \hat{d}_{ij}\, g(\mathbf{x}) \tag{4}$$
$$v_i(\mathbf{x}) = \hat{v}_i\, g(\mathbf{x}) \tag{5}$$
$$\psi(\mathbf{x}) = \hat{\psi}\, g(\mathbf{x}) \tag{6}$$

where $g(\mathbf{x})$ is a differentiable function and $\hat{d}_{ij}, \hat{v}_i, \hat{\psi}$ are constants. Substitution of (4)-(6) into (1) gives

$$\hat{d}_{ij}\frac{\partial}{\partial x_i}\left(g\frac{\partial c}{\partial x_j}\right) - \hat{v}_i\frac{\partial (gc)}{\partial x_i} = \hat{\psi} g\frac{\partial c}{\partial t} \tag{7}$$

Assume

$$c(\mathbf{x}, t) = g^{-1/2}(\mathbf{x})\,\sigma(\mathbf{x}, t) \tag{8}$$

therefore use of (4) and (8) in (2) gives

$$P(\mathbf{x}, t) = -P_g(\mathbf{x})\,\sigma(\mathbf{x}, t) + g^{1/2}(\mathbf{x})\,P_\sigma(\mathbf{x}, t) \tag{9}$$

where

$$P_g(\mathbf{x}) = \hat{d}_{ij}\frac{\partial g^{1/2}(\mathbf{x})}{\partial x_j}n_i \qquad P_\sigma(\mathbf{x}, t) = \hat{d}_{ij}\frac{\partial \sigma(\mathbf{x}, t)}{\partial x_j}n_i$$

Moreover, equation (7) can be written as

$$\hat{d}_{ij}\frac{\partial}{\partial x_i}\left[g\frac{\partial\left(g^{-1/2}\sigma\right)}{\partial x_j}\right] - \hat{v}_i\frac{\partial\left(g^{1/2}\sigma\right)}{\partial x_i} = \hat{\psi} g\frac{\partial\left(g^{-1/2}\sigma\right)}{\partial t}$$

$$\hat{d}_{ij}\frac{\partial}{\partial x_i}\left[g\left(g^{-1/2}\frac{\partial\sigma}{\partial x_j} + \sigma\frac{\partial g^{-1/2}}{\partial x_j}\right)\right] \\ -\hat{v}_i\left(g^{1/2}\frac{\partial\sigma}{\partial x_i} + \sigma\frac{\partial g^{1/2}}{\partial x_i}\right) = \hat{\psi} g\left(g^{-1/2}\frac{\partial\sigma}{\partial t}\right)$$

$$\hat{d}_{ij}\frac{\partial}{\partial x_i}\left(g^{1/2}\frac{\partial\sigma}{\partial x_j} + g\sigma\frac{\partial g^{-1/2}}{\partial x_j}\right) \\ -\hat{v}_i\left(g^{1/2}\frac{\partial\sigma}{\partial x_i} + \sigma\frac{\partial g^{1/2}}{\partial x_i}\right) = \hat{\psi} g^{1/2}\frac{\partial\sigma}{\partial t}$$

Use of the identity

$$\frac{\partial g^{-1/2}}{\partial x_i} = -g^{-1}\frac{\partial g^{1/2}}{\partial x_i}$$

implies

$$\hat{d}_{ij}\frac{\partial}{\partial x_i}\left(g^{1/2}\frac{\partial\sigma}{\partial x_j} - \sigma\frac{\partial g^{1/2}}{\partial x_j}\right) \\ -\hat{v}_i\left(g^{1/2}\frac{\partial\sigma}{\partial x_i} + \sigma\frac{\partial g^{1/2}}{\partial x_i}\right) = \hat{\psi} g^{1/2}\frac{\partial\sigma}{\partial t}$$

Rearranging and neglecting some zero terms gives

$$g^{1/2}\left(\hat{d}_{ij}\frac{\partial^2\sigma}{\partial x_i\partial x_j} - \hat{v}_i\frac{\partial\sigma}{\partial x_i}\right) \\ -\sigma\left(\hat{d}_{ij}\frac{\partial^2 g^{1/2}}{\partial x_i\partial x_j} + \hat{v}_i\frac{\partial g^{1/2}}{\partial x_i}\right) = \hat{\psi} g^{1/2}\frac{\partial\sigma}{\partial t}$$

So that if g satisfies

$$\hat{d}_{ij}\frac{\partial^2 g^{1/2}}{\partial x_i\partial x_j} + \hat{v}_i\frac{\partial g^{1/2}}{\partial x_i} - \lambda g^{1/2} = 0 \tag{10}$$

where λ is a constant, then the transformation (8) brings the variable coefficients equation (1) into a constant coefficients equation

$$\hat{d}_{ij}\frac{\partial^2\sigma}{\partial x_i\partial x_j} - \hat{v}_i\frac{\partial\sigma}{\partial x_i} - \lambda\sigma = \hat{\psi}\frac{\partial\sigma}{\partial t} \tag{11}$$

Taking the Laplace transform of (8), (9), (11) and applying the initial condition (3) we obtain

$$\sigma^*(\mathbf{x}, s) = g^{1/2}(\mathbf{x})\,c^*(\mathbf{x}, s) \tag{12}$$

$$P_{\sigma^*}(\mathbf{x}, s) = \left[P^*(\mathbf{x}, s) + P_g(\mathbf{x})\,\sigma^*(\mathbf{x}, s)\right]g^{-1/2}(\mathbf{x}) \tag{13}$$

$$\hat{d}_{ij}\frac{\partial^2\sigma^*}{\partial x_i\partial x_j} - \hat{v}_i\frac{\partial\sigma^*}{\partial x_i} - \left(\lambda + s\hat{\psi}\right)\sigma^* = 0 \tag{14}$$

By using Gauss divergence theorem, equation (14) can be transformed into a boundary integral equation

$$\eta(\boldsymbol{\xi})\;\sigma^*(\boldsymbol{\xi}, s) = \int_{\partial\Omega}\{P_{\sigma^*}(\mathbf{x}, s)\;\Phi(\mathbf{x}, \boldsymbol{\xi}) \\ -\left[P(\mathbf{x})\;\Phi(\mathbf{x}, \boldsymbol{\xi}) + \Gamma(\mathbf{x}, \boldsymbol{\xi})\right]\sigma^*(\mathbf{x}, s)\}\,dS(\mathbf{x}) \tag{15}$$

where

$$P_v(\mathbf{x}) = \hat{v}_i n_i(\mathbf{x})$$

For 2-D problems the fundamental solutions $\Phi(\mathbf{x}, \boldsymbol{\xi})$ and $\Gamma(\mathbf{x}, \boldsymbol{\xi})$ for are given as

$$\Phi(\mathbf{x}, \boldsymbol{\xi}) = \frac{\rho_i}{2\pi D}\exp\left(-\frac{\dot{\mathbf{v}}.\dot{\mathbf{R}}}{2D}\right)K_0\left(\dot{\mu}\dot{R}\right)$$
$$\Gamma(\mathbf{x}, \boldsymbol{\xi}) = \hat{d}_{ij}\frac{\partial\Phi(\mathbf{x}, \boldsymbol{\xi})}{\partial x_j}n_i$$

where

$$\dot{\mu} = \sqrt{(\dot{v}/2D)^2 + \left[\left(\lambda + s\hat{\psi}\right)/D\right]}$$
$$D = \left[\hat{d}_{11} + 2\hat{d}_{12}\rho_r + \hat{d}_{22}\left(\rho_r^2 + \rho_i^2\right)\right]/2$$
$$\dot{\mathbf{R}} = \dot{\mathbf{x}} - \dot{\boldsymbol{\xi}}$$
$$\dot{\mathbf{x}} = (x_1 + \rho_r x_2, \rho_i x_2)$$
$$\dot{\boldsymbol{\xi}} = (\xi_1 + \rho_r\xi_2, \rho_i\xi_2)$$
$$\dot{\mathbf{v}} = (\hat{v}_1 + \rho_r\hat{v}_2, \rho_i\hat{v}_2)$$
$$\dot{R} = \sqrt{(x_1 + \rho_r x_2 - \xi_1 - \rho_r\xi_2)^2 + (\rho_i x_2 - \rho_i\xi_2)^2}$$
$$\dot{v} = \sqrt{(\hat{v}_1 + \rho_r\hat{v}_2)^2 + (\rho_i\hat{v}_2)^2}$$

where ρ_r and ρ_i are respectively the real and the positive imaginary parts of the complex root ρ of the quadratic equation

$$\hat{d}_{11} + 2\hat{d}_{12}\rho + \hat{d}_{22}\rho^2 = 0$$

and K_0 is the modified Bessel function. Use of (12) and (13) in (15) yields

$$\eta(\boldsymbol{\xi})\;g^{1/2}(\boldsymbol{\xi})\;c^*(\boldsymbol{\xi}, s) \\ = \int_{\partial\Omega}\left\{\left[g^{-1/2}(\mathbf{x})\;\Phi(\mathbf{x}, \boldsymbol{\xi})\right]P^*(\mathbf{x}, s)\right. \\ + \left[\left(P_g(\mathbf{x}) - P_v(\mathbf{x})\;g^{1/2}(\mathbf{x})\right)\Phi(\mathbf{x}, \boldsymbol{\xi})\right. \\ \left.\left.-g^{1/2}(\mathbf{x})\;\Gamma(\mathbf{x}, \boldsymbol{\xi})\right]c^*(\mathbf{x}, s)\right\}dS(\mathbf{x}) \tag{16}$$

Equation (16) provides a boundary domain integral equation for determining the numerical solutions of c^* and its derivatives $\partial c^*/\partial x_1$ and $\partial c^*/\partial x_2$ at all points of Ω. The derivative solutions $\partial c^*/\partial\xi_1$ and $\partial c^*/\partial\xi_2$ can be determined using the following equations

$$\begin{aligned}\frac{\partial c^*(\boldsymbol{\xi},s)}{\partial\xi_1} &= \int_{\partial\Omega}\left\{\left[g^{-1/2}(\mathbf{x})\,\frac{\partial\Phi(\mathbf{x},\boldsymbol{\xi})}{\partial\xi_1}\right]P^*(\mathbf{x},s)\right.\\ &+\left[\left(P_g(\mathbf{x})-P_v(\mathbf{x})\,g^{1/2}(\mathbf{x})\right)\frac{\partial\Phi(\mathbf{x},\boldsymbol{\xi})}{\partial\xi_1}\right.\\ &\left.\left.-g^{1/2}(\mathbf{x})\,\frac{\partial\Gamma(\mathbf{x},\boldsymbol{\xi})}{\partial\xi_1}\right]c^*(\mathbf{x},s)\right\}dS(\mathbf{x})\\ &-c^*(\boldsymbol{\xi},s)\,\frac{\partial g^{1/2}(\boldsymbol{\xi})}{\partial\xi_1}\end{aligned}$$

$$\begin{aligned}\frac{\partial c^*(\boldsymbol{\xi},s)}{\partial\xi_2} &= \int_{\partial\Omega}\left\{\left[g^{-1/2}(\mathbf{x})\,\frac{\partial\Phi(\mathbf{x},\boldsymbol{\xi})}{\partial\xi_2}\right]P^*(\mathbf{x},s)\right.\\ &+\left[\left(P_g(\mathbf{x})-P_v(\mathbf{x})\,g^{1/2}(\mathbf{x})\right)\frac{\partial\Phi(\mathbf{x},\boldsymbol{\xi})}{\partial\xi_2}\right.\\ &\left.\left.-g^{1/2}(\mathbf{x})\,\frac{\partial\Gamma(\mathbf{x},\boldsymbol{\xi})}{\partial\xi_2}\right]c^*(\mathbf{x},s)\right\}dS(\mathbf{x})\\ &-c^*(\boldsymbol{\xi},s)\,\frac{\partial g^{1/2}(\boldsymbol{\xi})}{\partial\xi_2}\end{aligned}$$

Using the solutions $c^*(\mathbf{x},s)$ and its derivatives $\partial c^*/\partial x_1$ and $\partial c^*/\partial x_2$ obtained from reference (16), a numerical technique is used to perform a Laplace transform inversion. The Stehfest formula is employed to obtain the values of $c(\mathbf{x},t)$ and its derivatives $\partial c/\partial x_1$ and $\partial c/\partial x_2$. The Stehfest formula is

$$\begin{aligned} c(\mathbf{x},t) &\simeq \frac{\ln 2}{t}\sum_{m=1}^{N}V_m c^*(\mathbf{x},s_m)\\ \frac{\partial c(\mathbf{x},t)}{\partial x_1} &\simeq \frac{\ln 2}{t}\sum_{m=1}^{N}V_m\frac{\partial c^*(\mathbf{x},s_m)}{\partial x_1}\\ \frac{\partial c(\mathbf{x},t)}{\partial x_2} &\simeq \frac{\ln 2}{t}\sum_{m=1}^{N}V_m\frac{\partial c^*(\mathbf{x},s_m)}{\partial x_2}\end{aligned}\tag{17}$$

where

$$\begin{aligned} s_m &= \frac{\ln 2}{t}m\\ V_m &= (-1)^{\frac{N}{2}+m}\times\\ &\sum_{k=\left[\frac{m+1}{2}\right]}^{\min\left(m,\frac{N}{2}\right)}\frac{k^{N/2}(2k)!}{\left(\frac{N}{2}-k\right)!k!\,(k-1)!\,(m-k)!\,(2k-m)!}\end{aligned}$$

Possible multi-parameter solutions $g^{1/2}(\mathbf{x})$ to (10) are

$$g^{1/2}(\mathbf{x}) = \begin{cases}\text{constant}, \lambda=0\\ \exp(\beta_0+\beta_i x_i),\hat{d}_{ij}\beta_i\beta_j+\hat{v}_i\beta_i-\lambda=0\end{cases}\tag{18}$$

If the flow is incompressible, that is the divergence of the velocity is zero, then

$$\frac{\partial v_i(\mathbf{x})}{\partial x_i}=0$$

Therefore the governing equation (1) reduces to

$$\frac{\partial}{\partial x_i}\left[d_{ij}(\mathbf{x})\frac{\partial c(\mathbf{x},t)}{\partial x_j}\right]-v_i(\mathbf{x})\frac{\partial c(\mathbf{x},t)}{\partial x_i}=\psi(\mathbf{x})\frac{\partial c(\mathbf{x},t)}{\partial t}$$

Also, from (5) we obtain

$$\frac{\partial v_i(\mathbf{x})}{\partial x_i}=2g^{1/2}(\mathbf{x})\hat{v}_i\frac{\partial g^{1/2}(\mathbf{x})}{\partial x_i}=0$$

TABLE I

VALUES OF V_m OF THE STEHFEST FORMULA FOR $N = 8, 10, 12$

V_m	$N=8$	$N=10$	$N=12$
V_1	$-1/3$	$1/12$	$-1/60$
V_2	$145/3$	$-385/12$	$961/60$
V_3	-906	1279	-1247
V_4	$16394/3$	$-46871/3$	$82663/3$
V_5	$-43130/3$	$505465/6$	$-1579685/6$
V_6	18730	-236957.5	1324138.7
V_7	$-35840/3$	$1127735/3$	$-58375583/15$
V_8	$8960/3$	$-1020215/3$	$21159859/3$
V_9		164062.5	-8005336.5
V_{10}		-32812.5	5552830.5
V_{11}			-2155507.2
V_{12}			359251.2

so that

$$\hat{v}_i\frac{\partial g^{1/2}(\mathbf{x})}{\partial x_i}=0$$

Therefore equation (10) reduces to

$$\hat{d}_{ij}\frac{\partial^2 g^{1/2}}{\partial x_i\partial x_j}-\lambda g^{1/2}=0\tag{19}$$

Thus, for incompressible flow, possible multi-parameter functions $g^{1/2}(\mathbf{x})$ satisfying (19) are

$$g^{1/2}(\mathbf{x}) = \begin{cases}\beta_0+\beta_i x_i, \quad \text{if } \lambda=0\\ \cos(\beta_0+\beta_i x_i)+\sin(\beta_0+\beta_i x_i),\\ \qquad \text{if } \hat{d}_{ij}\beta_i\beta_j+\lambda=0\\ \exp(\beta_0+\beta_i x_i), \quad \text{if } \hat{d}_{ij}\beta_i\beta_j-\lambda=0\end{cases}\tag{20}$$

IV. NUMERICAL RESULTS

In this paragraph, the author describes some different test problems that will be considered to evaluate the effectiveness of the mixed Laplace transform-boundary element method (LT-BEM). Some of the problems have analytical solutions while others do not. The purpose of the tests is to validate the boundary integral equation (16), as well as to assess the accuracy, efficiency, and consistency of the mixed LT-BEM. The problems are governed by equation (1), and they satisfy specific initial and boundary conditions outlined in section II. The equation's coefficients, which represent the system's characteristics such as diffusivity, velocity, and change rate, are assumed to take specific forms. The author will use standard BEM to obtain numerical results. They will use a unit square (see Figure 1) with 320 equally sized elements and a FORTRAN script to perform the computations. Additionally, a subroutine to compute the Stehfest formula's coefficients for any even number N is included in the script, with Table I displaying the results for $N = 8, 10, 12$.

A. *A test problem*

The problem will consider three cases of inhomogeneity functions $g(\mathbf{x})$, namely exponential function of the form (18) for compressible flow, and quadratic or trigonometric functions taking the form (20) for incompressible flow. We take mutual coefficients $\hat{d}_{ij}$ and $\hat{v}_i$ for all test problems

$$\begin{aligned}\hat{d}_{ij} &= \begin{bmatrix}1 & 0.35\\ 0.35 & 0.65\end{bmatrix}\\ \hat{v}_i &= (1, 2.5)\end{aligned}$$

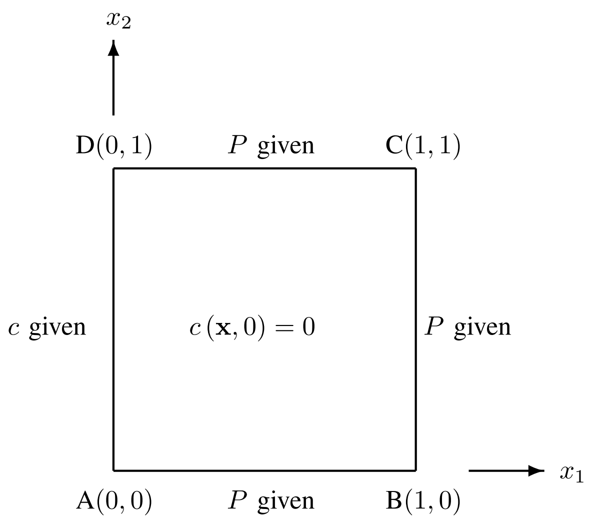

Fig. 1. The boundary conditions for Problem IV-A

and a mutual set of boundary conditions (see Figure 1)

P is given on side AB, BC, CD
c is given on side AD

For each case, numerical solutions for c and the derivatives $\partial c/\partial x_1$ and $\partial c/\partial x_2$ at 19×19 interior points which are $(x_1, x_2) = \{0.05, 0.1, 0.15, \ldots, 0.9, 0.95\} \times \{0.05, 0.1, 0.15, \ldots, 0.9, 0.95\}$ and 9 time-steps which are $t = 0.004, \frac{\pi}{8}, \frac{\pi}{4}, \frac{3\pi}{8}, \frac{\pi}{2}, \frac{5\pi}{8}, \frac{3\pi}{4}, \frac{7\pi}{8}, \pi$ are sought. The value $t = 0.004$ is the approximating value of $t = 0$ which is the singularity of the Stehfest formula (17). The relative error E of the numerical solutions are computed using the formulas

$$E = \left[\frac{\sum_{i=1}^{19\times19} (c_{n,i} - c_{a,i})^2}{\sum_{i=1}^{19\times19} c_{a,i}^2} \right]^{\frac{1}{2}}$$

where c_n and c_a are respectively the numerical and analytical solutions c or the derivatives.

Case 1:: First, we consider an example of an exponentially graded material and compressible flow with analytical solution

$$c(\mathbf{x}, t) = \frac{t \exp(-0.2x_1 + 0.3x_2)}{\exp(1 + 0.2x_1 - 0.1x_2)}$$

The gradation function is

$$g(\mathbf{x}) = [\exp(1 + 0.2x_1 - 0.1x_2)]^2$$

and the constant change rate is

$$\hat{\psi}^* = -0.476/s$$

From equation (10) we obtain the parameter

$$\lambda = -0.0175$$

Figure 2 shows the relative errors E of the numerical solutions c (top row), $\partial c/\partial x_1$ (middle row) and $\partial c/\partial x_2$ (bottom row). Each row of Figure 2 shows the errors E for $N = 8, 10, 12$. From Figure 2 we may say that the errors for the solution c are optimized when $N = 8$, $N = 10$ for the solutions $\partial c/\partial x_1$ and $\partial c/\partial x_2$. Table II shows the values of E when $N = 10$. According to Hassanzadeh and Pooladi-Darvish [21] increasing N will increase the accuracy up to a point, and then the accuracy will decline due to round-off errors.

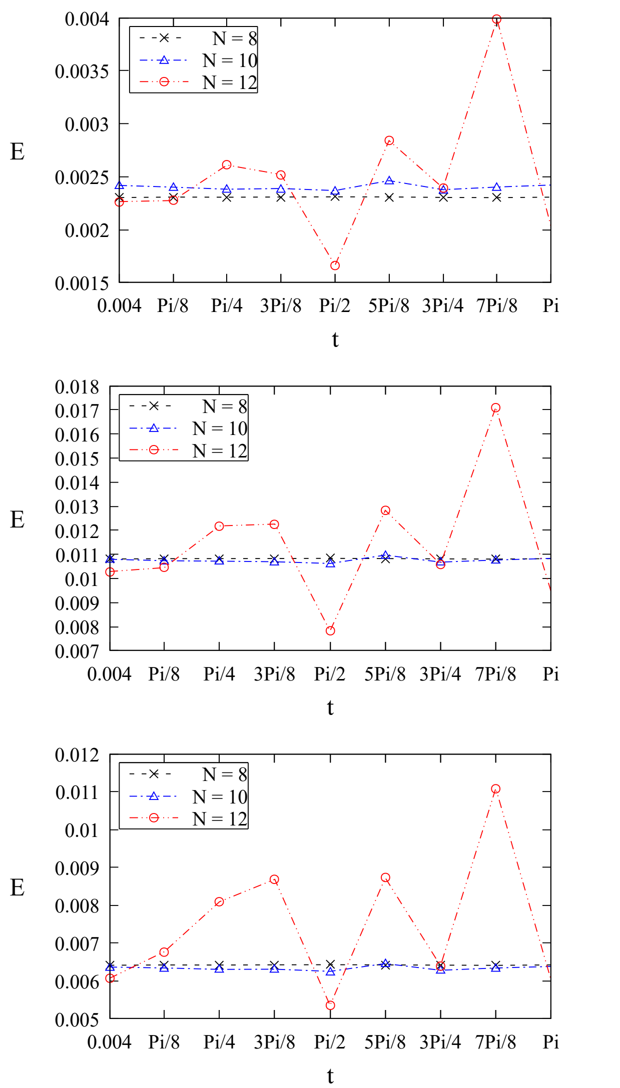

Fig. 2. The relative error E of the numerical solutions c (top row), $\partial c/\partial x_1$ (middle row) and $\partial c/\partial x_2$ (bottom row) for Case 1 with $N = 8, 10, 12$.

TABLE II
THE RELATIVE ERRORS E FOR NUMERICAL SOLUTIONS $c, \partial c/\partial x_1, \partial c/\partial x_2$ OF CASE 1 WITH $N = 10$

t	E		
	c	$\partial c/\partial x_1$	$\partial c/\partial x_2$
0.004	2.4180403E-003	1.0798660E-002	6.3669128E-003
$\pi/8$	2.4018083E-003	1.0738634E-002	6.3434275E-003
$\pi/4$	2.3821686E-003	1.0719655E-002	6.3051214E-003
$3\pi/8$	2.3888847E-003	1.0695628E-002	6.3102100E-003
$\pi/2$	2.3695990E-003	1.0624211E-002	6.2536332E-003
$5\pi/8$	2.4633840E-003	1.0971267E-002	6.4588734E-003
$3\pi/4$	2.3777798E-003	1.0680458E-002	6.2820693E-003
$7\pi/8$	2.4028151E-003	1.0766729E-002	6.3423626E-003
π	2.4216329E-003	1.0835465E-002	6.3829037E-003

Case 2:: Next, we consider an example for a quadratically graded material for which the gradation function is a quadratic function of the form

$$g(\mathbf{x}) = [1 + 0.25x_1 - 0.1x_2]^2$$

With this gradation function, the flow is incompressible and the parameter λ satisfying (19) is

$$\lambda = 0$$

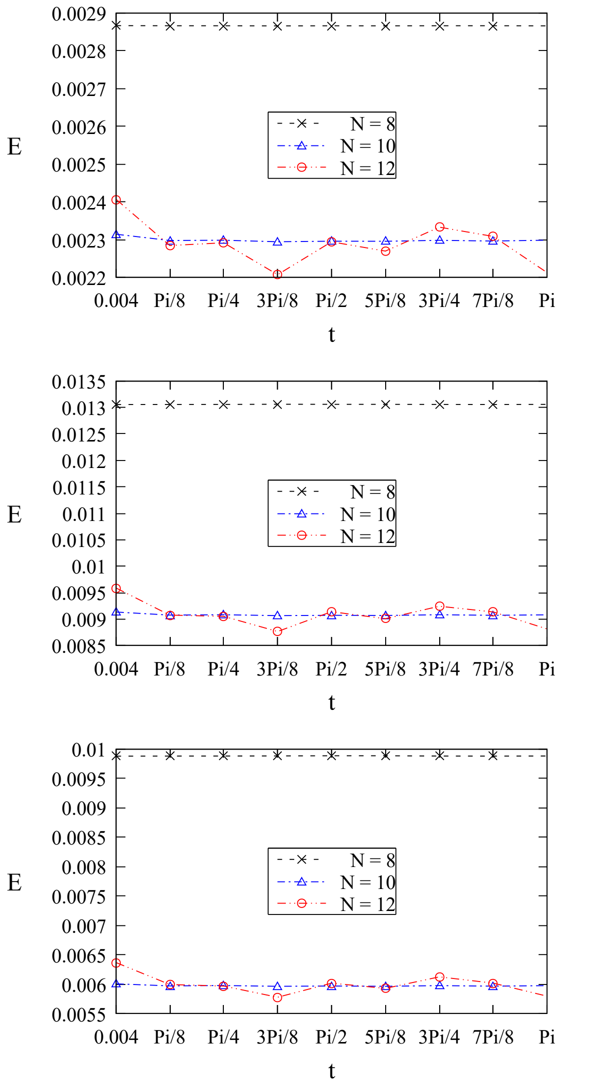

Fig. 3. The relative error E of the numerical solutions c (top row), $\partial c/\partial x_1$ (middle row) and $\partial c/\partial x_2$ (bottom row) for Case 2 with $N = 8, 10, 12$.

By taking the change rate

$$\hat{\psi}^* = -0.4935/s$$

the analytical solution is

$$c(\mathbf{x}, t) = \frac{t^2 \exp(-0.2x_1 + 0.3x_2)}{1 + 0.25x_1 - 0.1x_2}$$

Figure 3 shows the relative errors E of the numerical solutions c, $\partial c/\partial x_1$ and $\partial c/\partial x_2$. From Figure 3 we may take $N = 12$ as the optimized value for N for the solution c, and $N = 10$ for the solutions $\partial c/\partial x_1$ and $\partial c/\partial x_2$. Table III shows the values of E when $N = 10$.

Case 3:: Now we consider a system of a trigonometrically graded medium and incompressible flow with the following gradation function g, parameter λ, rate of change $\hat{\psi}$, and analytical solution

$$\begin{aligned} g(\mathbf{x}) &= [\cos(1 + 0.25x_1 - 0.1x_2)]^2 \\ \lambda &= -0.0515 \\ \hat{\psi}^* &= -0.442/s \\ c(\mathbf{x}, t) &= \frac{[1 - \exp(-t)] \exp(-0.2x_1 + 0.3x_2)}{\cos(1 + 0.25x_1 - 0.1x_2)} \end{aligned}$$

TABLE III
THE RELATIVE ERRORS E FOR NUMERICAL SOLUTIONS $c, \partial c/\partial x_1, \partial c/\partial x_2$ OF CASE 2 WITH $N = 10$

t	E		
	c	$\partial c/\partial x_1$	$\partial c/\partial x_2$
0.004	2.3148002E-003	9.1358617E-003	6.0087032E-003
$\pi/8$	2.2982990E-003	9.0784419E-003	5.9737613E-003
$\pi/4$	2.2990075E-003	9.0856284E-003	5.9803528E-003
$3\pi/8$	2.2950130E-003	9.0681408E-003	5.9667730E-003
$\pi/2$	2.2964343E-003	9.0745157E-003	5.9717345E-003
$5\pi/8$	2.2962355E-003	9.0710413E-003	5.9670842E-003
$3\pi/4$	2.2987712E-003	9.0857796E-003	5.9787878E-003
$7\pi/8$	2.2968682E-003	9.0742465E-003	5.9694806E-003
π	2.2991135E-003	9.0838460E-003	5.9783026E-003

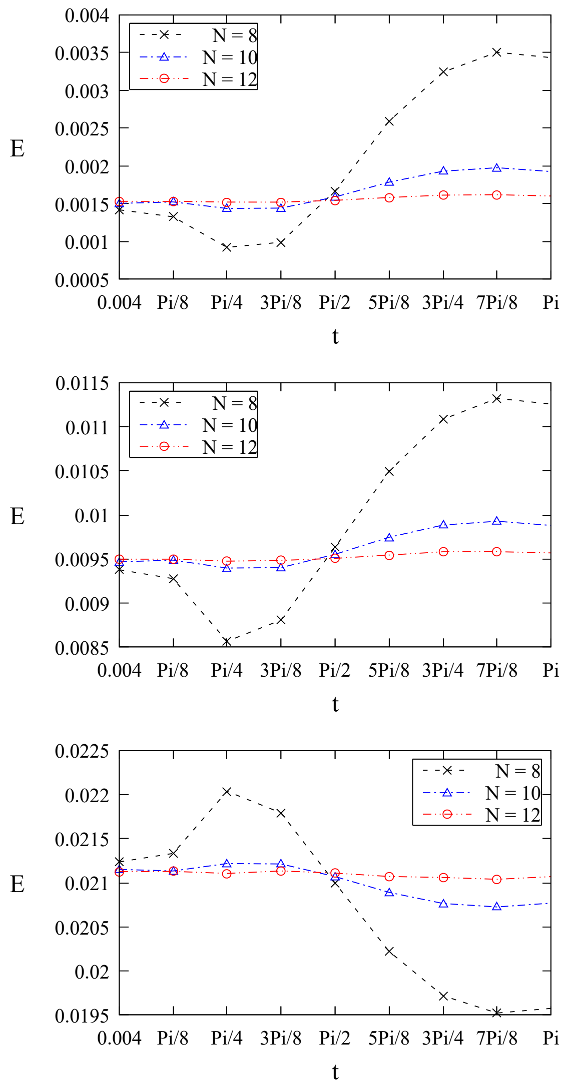

Fig. 4. The relative error E of the numerical solutions c (top row), $\partial c/\partial x_1$ (middle row) and $\partial c/\partial x_2$ (bottom row) for Case 3 with $N = 8, 10, 12$.

From Figure 4 it is obvious that $N = 12$ is the optimized value for the solutions c and $\partial c/\partial x_2$ and $N = 10$ for the solution $\partial c/\partial x_1$. Table IV shows the values of E when $N = 12$.

B. A problem without an analytical solution

A problem of an trigonometrically graded material will be considered. We take the constant coefficients $\hat{d}_{ij}, \hat{v}_i, \hat{\psi}$, a

TABLE IV
THE RELATIVE ERRORS E FOR NUMERICAL SOLUTIONS $c, \partial c/\partial x_1, \partial c/\partial x_2$ OF CASE 3 WITH $N = 12$

t	E		
	c	$\partial c/\partial x_1$	$\partial c/\partial x_2$
0.004	1.5324263E-003	9.4962887E-003	2.1124620E-002
$\pi/8$	1.5352355E-003	9.5083278E-003	2.1150117E-002
$\pi/4$	1.5412352E-003	9.4965120E-003	2.1094723E-002
$3\pi/8$	1.5584006E-003	9.5274502E-003	2.1111052E-002
$\pi/2$	1.4871866E-003	9.4516823E-003	2.1171840E-002
$5\pi/8$	1.2481136E-003	9.1806122E-003	2.1406095E-002
$3\pi/4$	9.6745092E-004	8.7730884E-003	2.1933828E-002
$7\pi/8$	9.8386442E-004	8.2603824E-003	2.2336695E-002
π	1.1195222E-003	8.1170979E-003	2.2754939E-002

gradation function $g(\mathbf{x})$ as follows

$$\begin{aligned} \hat{d}_{ij} &= \begin{bmatrix} 1 & 0.35 \\ 0.35 & 0.65 \end{bmatrix} \\ \hat{v}_i &= (1, 2.5) \\ \hat{\psi}^* &= 1/s \\ g(\mathbf{x}) &= [\cos(1 + 0.25x_1 - 0.1x_2)]^2 \quad \lambda = -0.0515 \end{aligned}$$

and a set of boundary conditions as shown in Figure 5 with cases of $P(t)$

Case 1: $P(t) = 10$
Case 2: $P(t) = 10t/(t + 0.01)$
Case 3: $P(t) = 10[1 - \exp(-t)]$

We will also consider the case when the material is homogeneous of constant gradation function

$$g(\mathbf{x}) = 1 \quad \lambda = 0$$

and the case of isotropic material with

$$\hat{d}_{ij} = \begin{bmatrix} 1 & 0 \\ 0 & 1 \end{bmatrix}$$

For all cases the parameter N for the Stehfest formula is 12.

Figures 6 and 7 show the results. Figure 6 indicates that the anisotropy and inhomogeneity of the material give effects on the values of c, as expected. Whereas Figure 7 shows that the solutions c at points $(0.5, 0.3), (0.5, 0.7)$ coincide when the material is isotropic homogeneous. This is expected as the problem is geometrically symmetric about the axis $x_2 = 0.5$ when the material is isotropic homogeneous. Moreover, the results in Figures 6 and 7 also indicate that for a pair of material's homogeneity and isotropy as t gets bigger the solution c tends to approach a same steady state value. For instance, when the material is anisotropic and homogeneous, the value of $c(0.5, 0.5, t)$ tends to approach 3.6 for the three cases of $P(t)$. This is also expected as the three forms of $P(t)$ will converge as t approaches infinity.

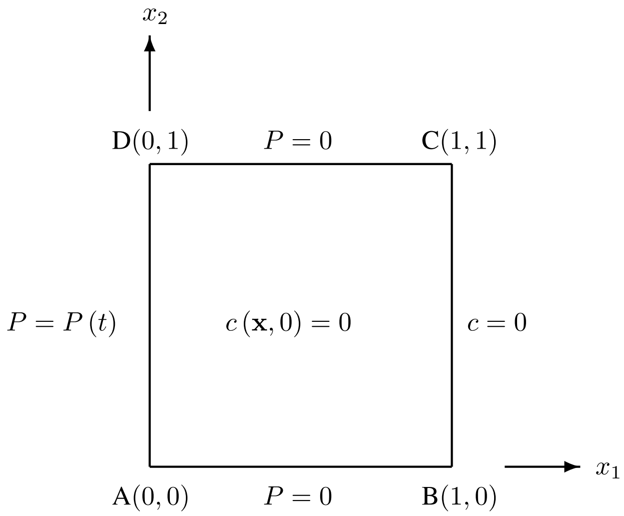

Fig. 5. The boundary conditions for Problem IV-B

V. CONCLUSION

The LT-BEM method has been successfully applied to solve initial boundary value problems for anisotropic functionally graded materials, using the transient DC equation (1) of compressible or incompressible flow. The method is simple to implement and avoids round-off errors, producing accurate solutions. By applying the method to three classes of functionally graded materials, it was found that the coefficients can depend on the same inhomogeneity or grading function, but it would be interesting to extend the study to coefficients that depend on different grading functions varying with time. To use the boundary integral equation (16), the boundary conditions need to be Laplace transformed, requiring an accurate technique for numerical Laplace transform inversion. The Stehfest formula was found to provide reasonably accurate solutions, as demonstrated by the results of the test problems.

REFERENCES

[1] M. Meenal, T. I. Eldho, "Two-dimensional contaminant transport modeling using mesh free point collocation method (PCM)," *Engineering Analysis with Boundary Elements*, vol. 36, pp. 551–561, 2012.

[2] F. Wang, W. Chen, A. Tadeu, C. G. Correia, "Singular boundary method for transient convection\textendash diffusion problems with time-dependent fundamental solution," *International Journal of Heat and Mass Transfer*, vol. 114, pp. 1126–1134, 2017.

[3] X-H. Wu, Z-J. Chang, Y-L. Lu, W-Q. Tao, S-P. Shen, "An analysis of the convection\textendash diffusion problems using meshless and mesh based methods," *Engineering Analysis with Boundary Elements*, vol. 36, pp. 1040–1048, 2012.

[4] H. Yoshida, M. Nagaoka, "Multiple-relaxation-time lattice Boltzmann model for the convection and anisotropic diffusion equation," *Journal of Computational Physics*, vol. 229, pp. 7774–7795, 2010.

[5] Q. Li, Z. Chai, B. Shi, "Lattice Boltzmann model for a class of convection-diffusion equations with variable coefficients," *Computers and Mathematics with Applications*, vol. 70, pp. 548–561, 2015.

[6] R. Pettres, L. A. de Lacerda, "Numerical analysis of an advective diffusion domain coupled with a diffusive heat source," *Engineering Analysis with Boundary Elements*, vol. 84, pp. 129–140, 2017.

[7] A. Rap, L. Elliott, D. B. Ingham, D. Lesnic, X. Wen, "DRBEM for Cauchy convection-diffusion problems with variable coefficients," *Engineering Analysis with Boundary Elements*, vol. 28, pp. 1321–1333, 1994.

[8] J. Ravnik, L. Škerget, "A gradient free integral equation for diffusion-convection equation with variable coefficient and velocity," *Eng. Anal. Boundary Elem.*, vol. 37, pp. 683–690, 2013.

[9] J. Ravnik, L. Škerget, "Integral equation formulation of an unsteady diffusion–convection equation with variable coefficient and velocity," *Computers and Mathematics with Applications*, vol. 66, pp. 2477–2488, 2014.

[10] C. Zoppou, J. H. Knight, "Analytical solution of a spatially variable coefficient advection-diffusion equation in up to three dimensions," *Appl. Math. Modell.*, vol. 23, pp. 667–685, 1999.

[11] N. La Nafie, M. I. Azis, Fahruddin, "Numerical solutions to BVPs governed by the anisotropic modified Helmholtz equation for trigonometrically graded media," *IOP Conference Series: Materials Science and Engineering*, vol. 619(1), 012058, 2019.

[12] M. I. Azis, S. Toaha, M. Bahri, N. Ilyas, "A boundary element method with analytical integration for deformation of inhomogeneous elastic materials," *J. Phys. Conf. Ser.*, vol. 979(1), 012072, 2018.

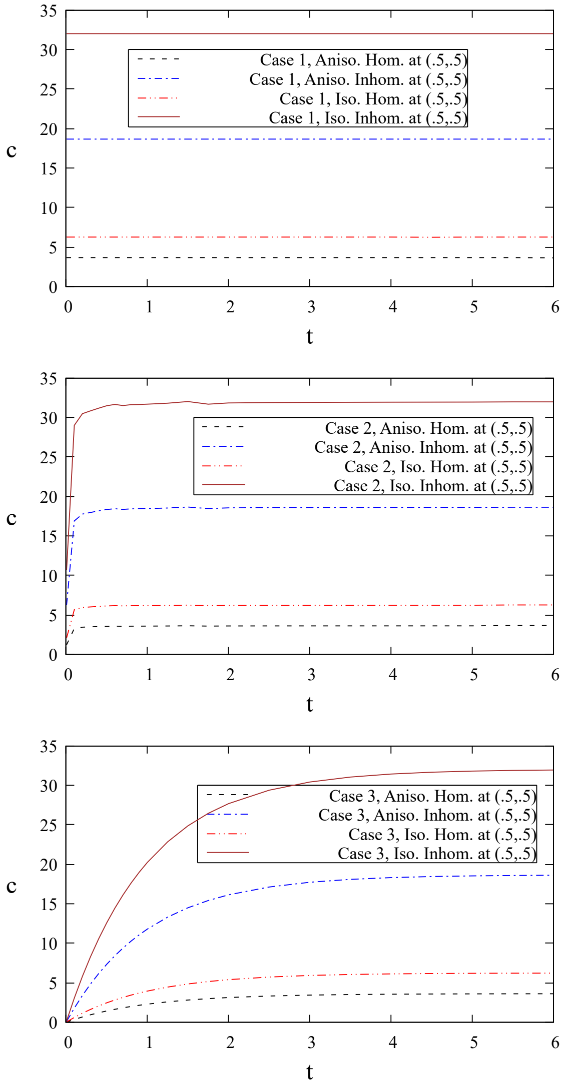

Fig. 6. Numerical solutions c at point $(0.5, 0.5)$ for Problem IV-B with $N = 12$.

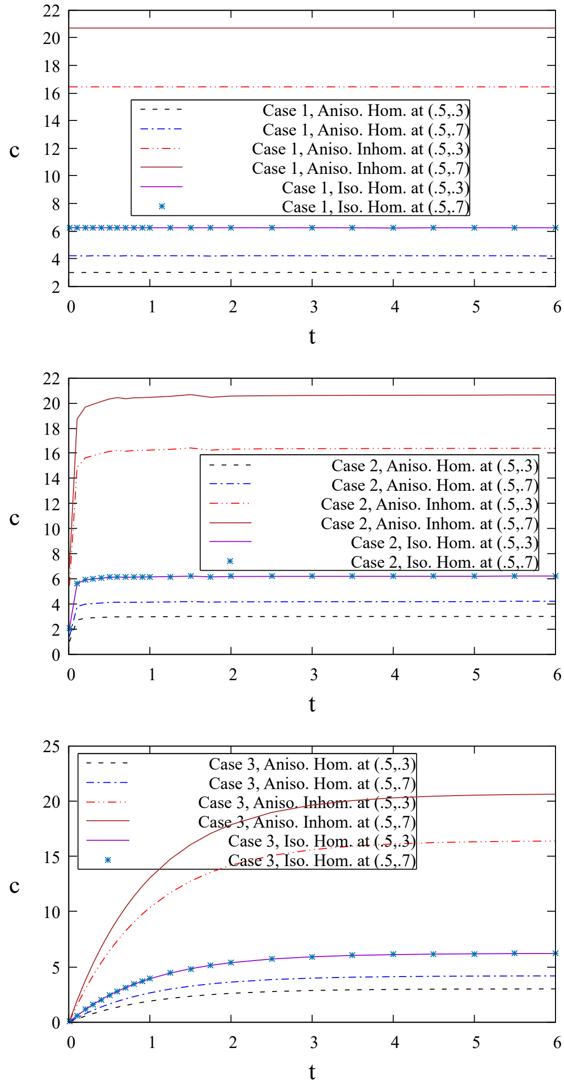

Fig. 7. Numerical solutions c at point $(0.5, 0.3)$, $(0.5, 0.7)$ for Problem IV-B with $N = 12$.

[13] M. I. Azis, "Numerical solutions to a class of scalar elliptic BVPs for anisotropic exponentially graded media," *J. Phys. Conf. Ser.*, vol. 1218(1), 012001, 2019.

[14] M. I. Azis, "A combined laplace transform and boundary element method for a class of unsteady laplace type problems of anisotropic exponentially graded materials," *Engineering Letters*, vol. 29(3), pp. 894–900, 2021.

[15] N. Lanafie, P. Taba, A. I. Latunra, Fahruddin, M. I. Azis, "On the derivation of a boundary element method for diffusion convection-reaction problems of compressible flow in exponentially inhomogeneous media," *J. Phys. Conf. Ser.*, vol. 1341, no. 6, pp. 062013, 2019.

[16] N. Rauf, H. Halide, A. Haddade, D. A. Suriamihardja, M. I. Azis, "A numerical study on the effect of the material's anisotropy in diffusion convection reaction problems," *J. Phys. Conf. Ser.* , vol. 1341, no. 8, pp. 082014, 2019.

[17] I. Raya, Firdaus, M. I. Azis, Siswanto, A. R. Jalil, "Diffusion convection-reaction equation in exponentially graded media of incompressible flow: Boundary element method solutions," *J. Phys. Conf. Ser.* , vol. 1341, no. 8, pp. 082004, 2019.

[18] N. Salam, D. A. Suriamihardja, D. Tahir, M. I. Azis, E. S. Rusdi, "A boundary element method for anisotropic-diffusion convection-reaction equation in quadratically graded media of incompressible flow," *J. Phys. Conf. Ser.*, vol. 1341, no. 8, pp. 082003, 2019.

[19] L. Zhou, M. Li, B. Chen, F. Li, X. Li, "An inhomogeneous cell-based smoothed finite element method for the nonlinear transient response of functionally graded magneto-electroelastic structures with damping factors," *Journal of Intelligent Material Systems and Structures*, vol. 30, pp. 416-437, 2019.

[20] L. Zhou, M. Li, W. Tian, P. Liu, "Coupled multi-physical cell-based smoothed finite element method for static analysis of functionally grade magneto-electro-elastic structures at uniform temperature," *Composite Structures*, vol. 226, 111238, 2019.

[21] H. Hassanzadeh, H. Pooladi-Darvish, "Comparison of different numerical Laplace inversion methods for engineering applications," *Appl. Math. Comput.*, vol. 189, pp. 1966–1981, 2007.